analytical chemistry

Article

Cite This: Anal. Chem. 2018, 90, 7544−7551

pubs.acs.org/ac

Fully Reversible Optical Sensor for Hydrogen Peroxide with Fast Response

Longjiang Ding, Siyu Chen, Wei Zhang, Yinglu Zhang, and Xu-dong Wang*

Department of Chemistry, Fudan University, 200433 Shanghai, People's Republic of China

Supporting Information

ABSTRACT: A fully reversible optical sensor for hydrogen peroxide with fast response is presented. The sensor was fabricated by in situ growing ultrasmall platinum nanoparticles (PtNPs) inside the pores of fibrous silica particles (KCC-1). The nanocomposite was then embedded into a hydrogel matrix and form a sensor layer, the immobilized PtNPs can catalytically convert hydrogen peroxide into molecular oxygen, which is measured via luminescent quenching based oxygen sensor underneath. Owing to the high porosity and permeability of KCC-1 and high local concentration of PtNPs, the sensor exhibits fast response (less than 1 min) and full reversibility. The measurement range of the sensor covers 1.0 μM to 10.0 mM, and a very small amount of sample is required during measurement (200 μL). Because of its high stability, excellent reversibility and selectivity, and extremely fast response, the sensor could fulfill all industry requirements for real-time measurement and fill market vacancy.

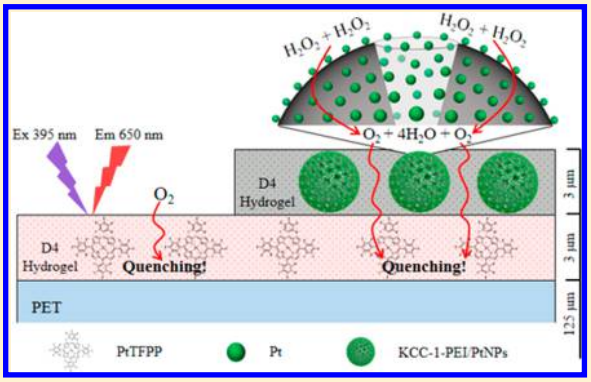

Hydrogen peroxide (H_2O_2), as an ecofriendly oxidant and reactant, has been widely used in the textile industry, for chemical bleaching, cleaning, and disinfecting, food processing, dechlorination, wastewater treatment, in gas scrubbers, and in cosmetic applications.[1] According to the latest statistics, almost 10000 tons of H_2O_2 is consumed daily.[2] However, recent research has revealed that excessive use or abnormal concentration of H_2O_2 is harmful to humans[3−5] and can cause environmental pollution and influence the biota ecosystem.[6] Up to now, to the best of our knowledge, there is no reliable monitoring system that can give real-time information on H_2O_2 concentration, which makes automatic and precise control of this chemical in industrial applications very difficult, especially in wastewater treatment, textile, and chemical bleaching industry, and in swimming pools. This is mainly because the state-of-the-art sensor technology for hydrogen peroxide has not satisfied reversibility, selectivity, and fast response time that can reach industry criteria. The currently commercially available sensors for H_2O_2 (DULCOTEST sensor) based on electrochemistry are not reliable, simply because they are cross-sensitive to many chemicals and interferences, such as chlorine dioxide, chlorine, bromine, ozone and so on. Therefore, there is an urgent demand to develop new methods and devices to measure H_2O_2 concentration in real time.

Classic method for determination of H_2O_2 is the photometric method using titanium sulfate, which was developed almost 100 years ago.[7−9] However, the response is irreversible and hardly leads to instrumentations. Researchers have developed other methods to measure H_2O_2,[1] which are mainly based on three different principles: (1) making use of the intrinsic physiochemical properties of H_2O_2, such as their Raman or infrared absorption feature; (2) exploring the oxidation power of H_2O_2; and (3) indirectly measuring the decomposed products of H_2O_2. Direct measuring H_2O_2 concentration is possible since the molecule has distinct Raman[10,11] (Raman shift 876 cm^{-1}) and infrared[12] (2930−2680, 1530−1260, and 890−800 cm^{-1}) absorption. However, the absorption spectra of many molecules, including water and most biomolecules, severely overlapped with that of H_2O_2, which strongly interferes direct H_2O_2 measurement. The widely used electrochemical approach faces the same interference problems.[13,14]

Alternatively, H_2O_2 can be sensed by exploring its oxidative power. H_2O_2 can oxide certain chemicals such as bis(2,4,5-trichloro-6-carbopentoxy-phenyl) oxalate (CPPO) to generate chemiluminescence,[15,16] which is long known as the chemistry of glow sticks. By measuring the chemiluminescent intensity, the concentration H_2O_2 can be measured. The method is very sensitive because of its extremely low background. However, the chemiluminescence generation process is irreversible, which cannot result in instrumentation that can measure its concentration in real time. Some organic dyes (e.g., 4-nitrophenyl boronic acid)[17] and metal nanoparticles (such as silver nanoparticles)[18−20] can be oxidized by H_2O_2, which is in concomitant with apparent color changes and can be explored for semiquantitatively measuring the concentration of H_2O_2. In addition, Meldola Blue,[21] EuTC,[5,22] and Eu^{3+}-doped $GdVO_4$

Received: March 14, 2018
Accepted: May 9, 2018
Published: May 9, 2018

DOI: 10.1021/acs.analchem.8b01159
Anal. Chem. 2018, 90, 7544−7551

nanocrystals[23] can react with H_2O_2 and cause changes in luminescence intensities, which are employed for sensing the chemical. Besides, H_2O_2 can be reduced using strong oxidizing agent, such as $KMnO_4$, and the reaction has been used for H_2O_2 titration.[24] However, the redox-reaction based H_2O_2 sensors are suffering from their irreversible nature, which are suitable for one-shot measurement, but cannot fit the industrial standard for real-time monitoring.

In order to solve the obstacle, researchers have developed an indirect approach for H_2O_2 sensing. As a common sense, H_2O_2 can be catalytically decomposed into oxygen and water. The measurement of water molecules in aqueous solution is nearly impossible. In contrast, the produced oxygen can separate from aqueous phase, and accumulate to form big bubble that can be sensitively measured using gasometer based on weighing,[25] pressure meter,[26,27] or oxygen sensors.[28,29] The gasometer based on weighing and the pressure meter are not sensitive enough, and confined space are required during measurement, which strongly limited their application as online sensors for H_2O_2. The electrochemical oxygen sensor is not suitable to be integrated for indirect H_2O_2 sensing due to its feature of oxygen consumption and requirement of constant stirring.[30] Due to its outstanding characteristics, optical oxygen sensors based on luminescence quenching have been chosen as an ideal indirect way to measure H_2O_2. Posch and Wolfbeis developed the first proof of the concept optical H_2O_2 sensor in 1989,[31] which consists of a H_2O_2-catalyst layer using silver powder and an oxygen-sensor layer using $Ru(dipy)_3Cl_2$. The sensor is fully reversible and can measure H_2O_2 concentration in the range of 0.1 to 10 mM. However, due to the limited catalytical capability of silver powder and inadequate oxygen sensitivity of $Ru(dipy)_3Cl_2$ dye, the sensor exhibits a long response time (~5 min) and is only suitable for measuring H_2O_2 at high concentration. Inspired by this pioneering work, intensive efforts have been devoted to improve sensor performance, including adjusting sensor film structure,[32] using more sensitive probe for oxygen,[22] and screening more efficient catalyst for H_2O_2 decomposition.[33] However, there is no significantly breakthrough until now, and the sensor still has poor stability (due to dye and catalyst leaching, catalyst poisoning), limited sensitivity, long response time (>5 min), and unsatisfied reversibility.

Herein, we have developed a highly sensitive, fully reversible, and reliable optical sensor for H_2O_2, with fast response and excellent stability. Highly sensitive oxygen sensor film was integrated with an ultrastable and highly efficient catalytical layer to form a sensor film, which can rapidly convert H_2O_2 into oxygen. The concentration of decomposed oxygen was sensitively measured by a luminescence-quenching-based oxygen sensor. Owing to our in situ growth strategy and the rational-designed nanostructure, the sensor exhibits extremely high stability over long time without observed loss of performance. The specially designed fibrous nanostructure also largely enriched catalyst concentration in the sensor film, which ensures the sensor having fast response (<1 min), good stability, and full reversibility. Because of the simplicity of the sensor design, the new H_2O_2 sensor is fully compatible with all commercial-available optical oxygen sensor devices, which makes the application of such sensors much easier and more economically friendly.

EXPERIMENTAL SECTION

Reagents and Instruments. Hydrogen peroxide (27%) were purchased from Alfa Aesar (www.thermofisher.com). Potassium tetrachloroplatinate(II) (K_2PtCl_4), sodium borohydride ($NaBH_4$), tetraethyl orthosilicate (TEOS), polyethylenimine branched (PEI, $M_w \sim 800$) were bought from Sigma-Aldrich (www.sigmaaldrich.com). Hydrogel-type D4 were purchased from Cardiotech Intl. Inc. Hydrogen hexachloroplatinate(IV) hexahydrate ($H_2PtCl_6 \cdot 6H_2O$), L-ascorbic acid (AA), hexadecylpyridinium bromide hydrate (CPB), 3-glycidyloxypropyl)-trimethoxysilane (GTMS), sodium chloride (NaCl), potassium bromide (KBr), sodium sulfate (Na_2SO_4), urea, glucose, cyclohexane, and pentanol were obtained from TCI (Shanghai) Development Co., Ltd. (www.tcichemicals.com). Platinum(II) meso-tetra(pentafluorophenyl)porphine (PtTFPP) was synthesized by Heowns (www.heowns.com). Tetrahydrofuran (THF) were purchased from Adamas Reagent Co., Ltd. (www.adamas-beta.com). PET membrane was manufactured by Goodfellow (www.goodfellow.com, U.K.). All chemicals were of analytical grade and used as received without further purification. Deionized (DI) water was used throughout all experiments.

The morphology and size of obtained samples was characterized using a Field Emission Transmission Electron Microscopy (TEM, FEI Tecnai G2 F20 S-Twin). Their compositions were studied using an energy-dispersive X-ray spectroscopy (EDX, Nova NanoSem 450). The luminescence spectra were recorded using a Hitachi F7000 fluorescence spectrometer.

Preparation of Pt Nanoparticles (PtNPs). The PtNPs were synthesized via an aqueous route.[27] Typically, 100 μL of freshly prepared ascorbic acid solution (0.4 M) was added to 1.0 mL of H_2PtCl_6 solution (1.0 mM) and immediately incubated at 80.0 °C for 30 min. After centrifugation, the obtained PtNP solution (0.15 mg mL^{-1}) were stored at 4.0 °C before use.

Preparation of Fibrous Nanosilica (KCC-1). The fibrous nanosilica KCC-1 was synthesized using a microwave-assisted hydrothermal technique according to a previous report[34,35] with necessary adaption. CPB (1.0 g, 2.6 mmol) and urea (0.6 g, 10 mmol) were continuously stirred (1200 rpm) in DI water (30 mL) until forming a white suspension. TEOS (2.7 mL, 12 mmol) was added to a mixture containing 30 mL of cyclohexane and 1.5 mL of pentanol. Next, the prepared white suspension was added dropwisely to the above-mentioned mixture and stirred for 30 min at room temperature. The resulting mixture was then transferred to a Teflon-lined stainless steel autoclave (100 mL), sealed and reacted at 120.0 °C for 4 h. The solution was then cooled to room temperature after hydrothermal treatment, followed by centrifuging at 15000 g to isolate the particles. The obtained particles were washed with ethanol and DI water for at least 3 times. After drying in air for 2 h, the sample was finally calcined at 550 °C in air for 6 h.

In Situ Growth of PtNPs in Fibrous KCC-1 Particle. The PtNP-doped KCC-1 particle was synthesized by directly growing PtNPs in situ,[36] for which, the inner-channel surface of KCC-1 particle needs to be modified with positively charged group to facilitate the attachment of PtNPs. In a typical procedure, 0.4 g KCC-1 particle was degassed in vacuum at 120 °C for 16 h and cooled to 60 °C. After adding 2.4 mL of hot methanol (60 °C) along with 0.44 g GTMS (1.9 mmol), the

DOI: 10.1021/acs.analchem.8b01159
Anal. Chem. 2018, 90, 7544−7551

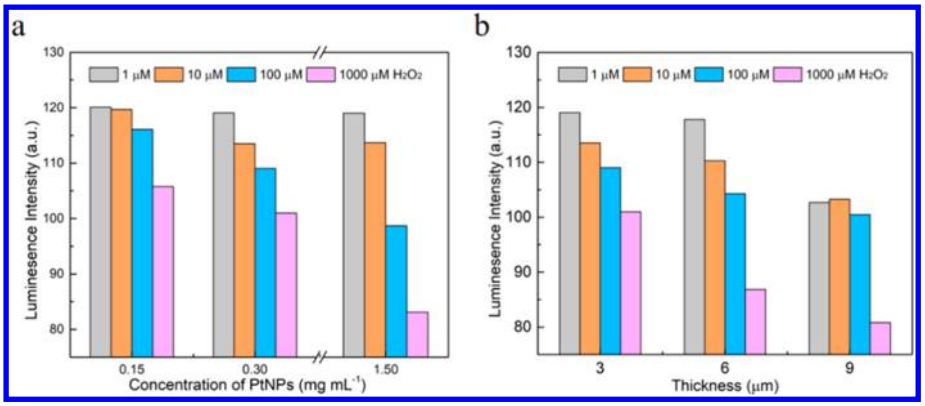

Figure 1. Response of sensor films with different concentration of PtNPs (a) and thickness of catalyst layer (b) at different concentrations of H_2O_2 marked in color. The sensor performance was improved by increasing the concentration of PtNPs and using thicker film. However, the sensor performance will decrease when the thickness of catalyst layer reach to 9.0 μm.

reaction mixture was kept stirring for 1.5 h at 60 °C. The procedure was followed by adding another portion of hot methanol (2.4 mL) containing 0.36 g PEI (0.45 mmol). The particle suspension was continuously stirred at 60 °C for 5 h. The PEI-modified particles were then harvested by centrifugation and washed with hot methanol for three times. After drying at 80 °C in vacuum for 12 h, 200.0 mg of the obtained KCC-1-PEI was suspended into 20 mL DI water, which was then sonicated for 5 min and vigorously stirred for 10 min at room temperature to disperse the particles uniformly.

To grow PtNPs directly in the channel of KCC-1-PEI particle, 4.0 mL of aqueous solution of K_2PtCl_4 (25 mM) was dropwisely added in the particle suspension, sonicated for 30 min, and stirred at room temperature for 2 h. The K_2PtCl_4 was reduced in situ by dropwise adding 2.0 mL of freshly prepared $NaBH_4$ solution (1.0 M in DI water), followed by continuously stirring for 2 h at room temperature. Finally, PtNP decorated KCC-1 particles were harvested by centrifugation at 15000 g and washed with DI water and ethanol for three times, respectively. After drying under vacuum at 80 °C for 16 h, the KCC-1-PEI/PtNPs were ready to use.

Fabrication of the H_2O_2 Sensors. The optical sensor film for H_2O_2 was fabricated using a homemade knife-coating device, which was a multilayer film, and composed of a transparent PET foil as solid support, an oxygen-sensitive layer, and a H_2O_2-catalyst layer. A solution of 5% polyurethane D4 hydrogel prepared in 90% ethanol was used as polymer matrix to incorporate both the oxygen-sensitive dye PtTFPP and the KCC-1-PEI/PtNPs. The D4 hydrogel was mixed with PtTFPP solution (2.0 mg mL^{-1} in THF) with a volume ratio at 1:4 to form a cocktail, and then the cocktail was knife-coated onto the PET foil with a wet thickness of 125 μm to form the oxygen-sensitive layer. The H_2O_2-catalyst layer was formed by coating the mixture of 10 mg KCC-1-PEI/PtNPs and 500 μL of 5% D4 hydrogel onto the dried oxygen-sensitive layer with a wet thickness of 125 μm. The obtained sensor film was dried at room temperature and was then ready to use. The dried thickness of the H_2O_2-catalyst layer and the oxygen-sensor layer was about 3.0 μm.

RESULT AND DISCUSSION

Our new optical sensor for H_2O_2 was constructed using a transparent PET foil as mechanical support, followed by coating an oxygen-sensitive layer and a layer of catalyst that converts H_2O_2 into molecular oxygen. The PtTFPP in hydrogel was used as oxygen sensing materials because of their high sensitivity, good mechanical, and optical stability, as well as high flexibility for integrating with other sensors.[29,37] In order to construct a sensor for H_2O_2 with high sensitivity and fast response, an obvious solution is to increase both the speed and the amount of oxygen generation, which is highly depending on the catalytical capability of the catalyst layer. The use of silver nanoparticles,[31] catalase,[31] and RuO_2[33] as catalyst in the literature do not result in sensors with good sensitivity and fast response, because these materials only have limited catalytical activity and cannot generate adequate oxygen in a short time. They also face a problem that these materials tend to leach from sensor film. The use of biomaterials as catalyst further causes problems in long-term stability and short shelf life. Thus, increasing the capability of catalyst is a straightforward approach to solve all problems.

Inspired by a very recently report that PtNPs can generate 400× as much oxygen per second as catalase due to their inherent high catalytic efficiency and long lifespan.[27] Our first attempt was trying to immobilize PtNPs directly in hydrogel as much as possible. We first synthesized PtNPs in solution at a concentration of 0.15 mg mL^{-1}, mixed with D4 hydrogel, and coated on the oxygen-sensitive film to form the H_2O_2-catalyst layer. The performance of the sensor film was characterized on a fluorescence spectrometer with excitation wavelength set at 395 nm to maximally excite the PtTFPP dye. The emission of PtTFPP dye peaked at 650 nm was selected to study the time response of the sensor film (Figure S1, Supporting Information). Results show that there is an apparent decreasing in luminescence intensity with the addition of H_2O_2 at a concentration of 1.0 mM, which indicated that the immobilized PtNPs can catalytically convert H_2O_2 into oxygen and quenches the luminescence of oxygen sensor. However, the PtNP-based H_2O_2 sensor exhibited poor stability and long response time (>6.0 min, Figure S2). The reversibility test shows that the sensor could reversibly response to H_2O_2. However, there is a 12.0% loss of its initial intensity during the first circle (Figure S2). Since PtTFPP dye shows excellent photostability during measurement,[38,39] the loss in luminescence intensity was due to the leakage of PtNPs during continuous measurement. In addition, the sensor is not sensitive enough to measure low concentration of H_2O_2.

As shown in Figure 1a and Figure S3 in the Supporting Information, with the increasing of PtNPs concentration, the sensor exhibits improved response and better sensitivity.

DOI: 10.1021/acs.analchem.8b01159
Anal. Chem. 2018, 90, 7544−7551

However, the sensitivity is still not good enough to resolve low concentration of H_2O_2 (1.0−10 μM), even when the PtNPs concentration reached as high as 1.5 mg mL^{-1}. Further enrichment of PtNPs using centrifugation causes severe aggregation of PtNPs, and seriously influences their catalytical performances. The use of thicker catalyst layer can also improve sensor sensitivity to some extent (Figures 1b and S4). However, further increasing the dried film thickness to 9.0 μm results in decreases in sensitivity, because the catalyst layer is so thick that the diffusion of produced molecular oxygen to the oxygen-sensitive layer is influenced. All these results show that improves in the performance of the catalyst layer is the right direction to fabricate highly sensitive H_2O_2 sensor. However, simple solutions, such as increasing concentration of PtNPs and the thickness of catalyst layer, could not lead to optimum sensor for H_2O_2. The leakage of catalyst during measurement is also one of the major contributions to the poor stability and reversibility of current H_2O_2 sensor.

The rapid development of nanotechnology has offered us the opportunity to further increase the local concentration of catalyst by designing porous structure. The porous structure not only provides much large surface area, but also offers space to immobilize catalyst. Catalyst anchored in/on porous materials could greatly increase the local concentration of catalyst, and at the same time, the composite structure could prevent leakage of catalyst, which ensures good stability over long-term use. The search of porous particle with large-enough pores that can anchor smaller metal nanoparticles has resulted in a new class of fibrous nanosilica, named KCC-1.[34,35] The material features excellent physical properties, including high surface area, large pores (8−10 nm), fibrous morphology, high mechanical stability and good thermal/hydrothermal properties.[35] The large pores enable direct growth of metal nanoparticles (such as Pd, Ru, and Rh) inside, and the resulting composite materials have been proved to have a multifold increase in their catalytic efficiency and stability.[40,41] The KCC-1 particles not only act as a carrier for metal nanoparticles, but also disperse them uniformly to prevent aggregation and leaching.

The PtNPs decorated KCC-1 particles were synthesized in three steps (Scheme 1). The KCC-1 particles are formed according to a hydrothermal approach with proper adaption. The obtained KCC-1 particles are calcined to remove surfactant, and then their surface (including fibrous pore surface) is functionalized with positively charged PEI. This modification process is critical for the in situ growth of PtNPs. The TEM images (Figure 2a) show that agglomeration-free KCC-1 particles were obtained, and their average size was about 500 nm. Figure 2b shows the fibrous structure of the silica particles, and numerous fiber channels (V-shape pores), were distributed on the particles at high density, which would largely increase the surface area. The calcination process removes the template during synthesis, and the void space in the channels enables the growth of small metal particles inside. In addition, the large porous structure is beneficial to the diffusion of the reactant in and out of the channels.

In order to highly accumulate PtNPs in the porous channels of the KCC-1 particles, the surface of KCC-1 particles is needed to be modified with positively charged PEI. Our attempt to grow PtNPs in solution with the presence of KCC-1 particle failed. As shown in Figure S5 in the Supporting Information, the PtNPs prefer to form larger aggregates rather than distribute in the fibrous channel of KCC-1 particle. Due to

Scheme 1. Synthesis Process of the KCC-1-PEI/PtNPs[a]

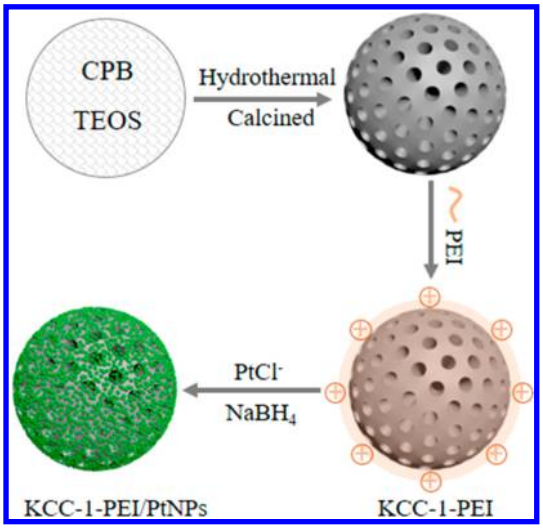

[a]The KCC-1 bare particles are first functionalized with positively-charged PEI, and then PtNPs are grown inside the V-shape pores of KCC-1 particles by an in situ reduction reaction.

the negatively charged surface silanol groups on silica particles,[42] the inner channel presents high repulse force to the anion $PtCl_4^-$. Few, if any, platinum anions are present in the channel, which makes nucleation to form PtNPs difficult. In contrast, the introduction of positively charged multibranch PEI on KCC-1 particle surface creating a covalently linked hydroxy-polyamine branched network,[36] which attracts negatively charged platinum anions inside the fibrous channel. Then, PtNPs can be reduced directly in the channel of modified KCC-1-PEI particles, resulting in uniformly distributed PtNPs in KCC-1-PEI particles (Figure 2c). The average particle size of PtNPs is approximately 2 nm (Figures 2d and S6). The multiple amine groups on PEI molecule bind strongly with PtNPs and make them hardly detached from the surface of KCC-1 particle. The element mapping of a single KCC-1-PEI/PtNPs (Figure 3) shows that PtNPs are uniformly distributed throughout the KCC-1 particles. The calculation shows that 10.19% of the full weight of composite particle is platinum, indicating that a large amounts of PtNPs are uniformly distributed in the KCC-1 particles (Figure S7). The rationally designed structure not only drastically increases the local concentration of PtNPs, but also maximally retains the mechanical stability and prevents leakage and aggregation of PtNPs catalyst. All these features guarantee the good stability and reversibility of the H_2O_2 sensor.

The synthesized KCC-1-PEI/PtNPs composite materials was then immobilized in hydrogel at a large concentration of 20.0 mg mL^{-1} and coated on the oxygen-sensitive layer to form our new H_2O_2 sensor (Scheme 2). Because the PtNPs are distributed in the KCC-1 particles, a large concentration of the composite materials can be used to prepare thin film for sensing H_2O_2 without worrying about aggregation of PtNPs. Thin film is beneficial for molecules diffusion and can significantly reduce response time. The immobilized high concentration of PtNPs can quickly decompose H_2O_2 into oxygen and form a large quantity of molecular oxygen in a short time. The produced oxygen was rapidly diffused into the oxygen-sensitive layer, and its concentration was quantitatively

DOI: 10.1021/acs.analchem.8b01159
Anal. Chem. 2018, 90, 7544−7551

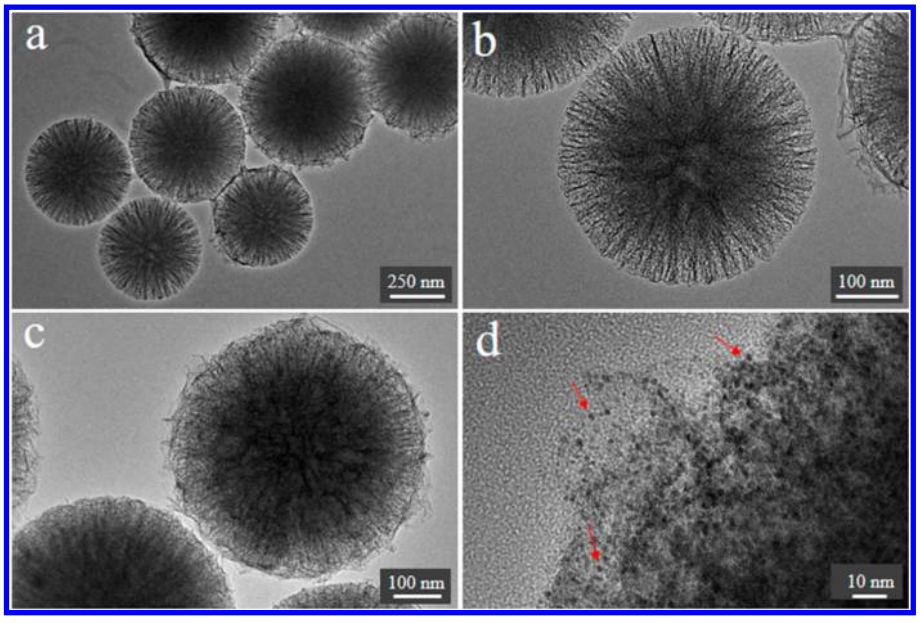

Figure 2. TEM images of bare KCC-1 particles (a, b) and PtNPs-decorated KCC-1 particles (c, d) with low (left) and high (right) magnification. The V-shape pores can be clearly seen in the magnified pictures, and PtNPs (shown with red arrow) are uniformly distributed inside the pores (d).

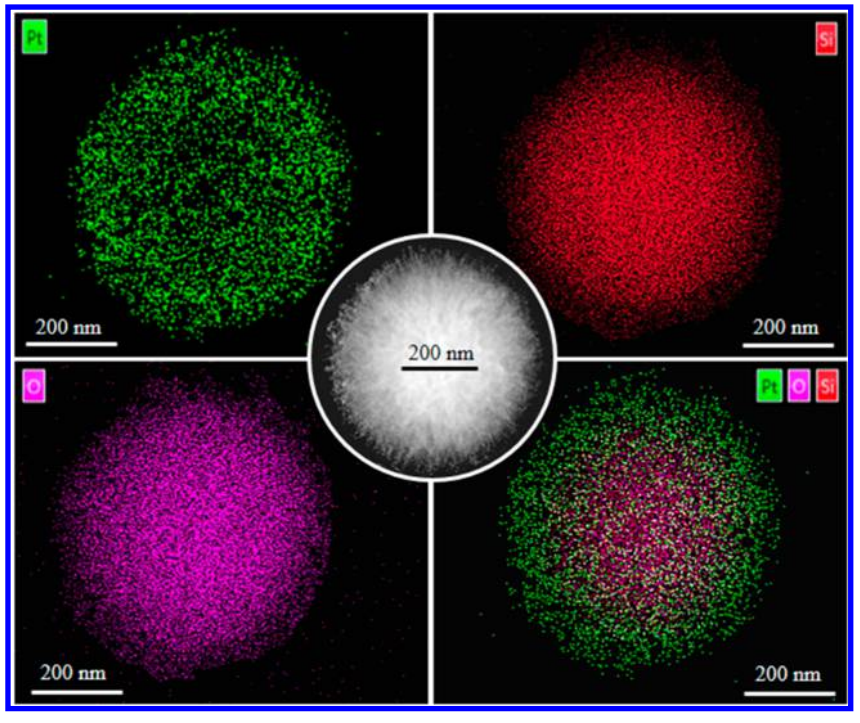

Figure 3. EDX element mapping images of the elements Pt, Si, and O in a single KCC-1-PEI/PtNPs. From the Pt (green color) and Si (red color) mapping images, it is clear that PtNPs are uniformly distributed throughout the entire KCC-1 particle.

measured by the optical oxygen sensor based on luminescence quenching.

Finally, the performance of our H_2O_2 sensor was fully characterized using a homemade flow-through cell. The sensor film was placed inside the cell and different concentration of H_2O_2 was pumped in the cell using a peristaltic pump. The sensor film was excited at wavelength of 395 nm and the emission of PtTFPP peaked at 650 nm was recorded using a fluorescence spectrometer. Results summarized in Figure 4a show that luminescence intensity obviously decreased with increasing H_2O_2 concentration. The sensor exhibits good sensitivity in the concentration range from 1.0 μM to 10.0 mM, and the detection limit is 15 μM (S/N = 3). The calibration curve (Figure 4b) fits well with the Stern−Volmer equation and the two-site model could be applied to achieve Stern−Volmer parameters.[31,33] Owing to the high local concentration of PtNPs, the sensor shows very fast response. As shown in Figure 4c, the t_{95} of the sensor responding to 3.0 mM of H_2O_2 is less than 1 min, which is much faster than previous reports (Table 1). More importantly, the sensor exhibits excellent reversibility and stability as shown in Figure 4d. Continuous switching the test sample from 1.0 M H_2O_2 to H_2O, the sensor shows fully

DOI: 10.1021/acs.analchem.8b01159
Anal. Chem. 2018, 90, 7544−7551

Scheme 2. Working Principle of KCC-1-PEI/PtNPs Based H_2O_2 Sensor[a]

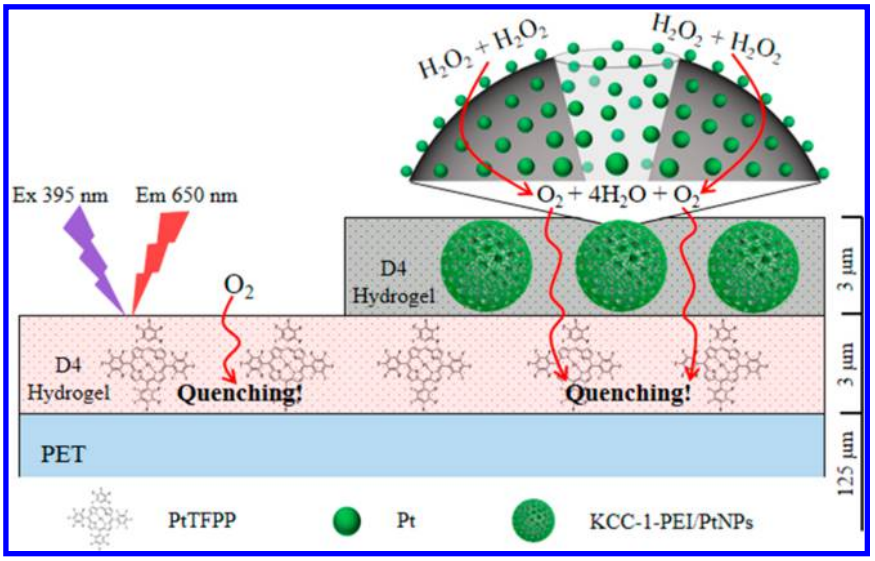

[a]The picture is not drawn to scale.

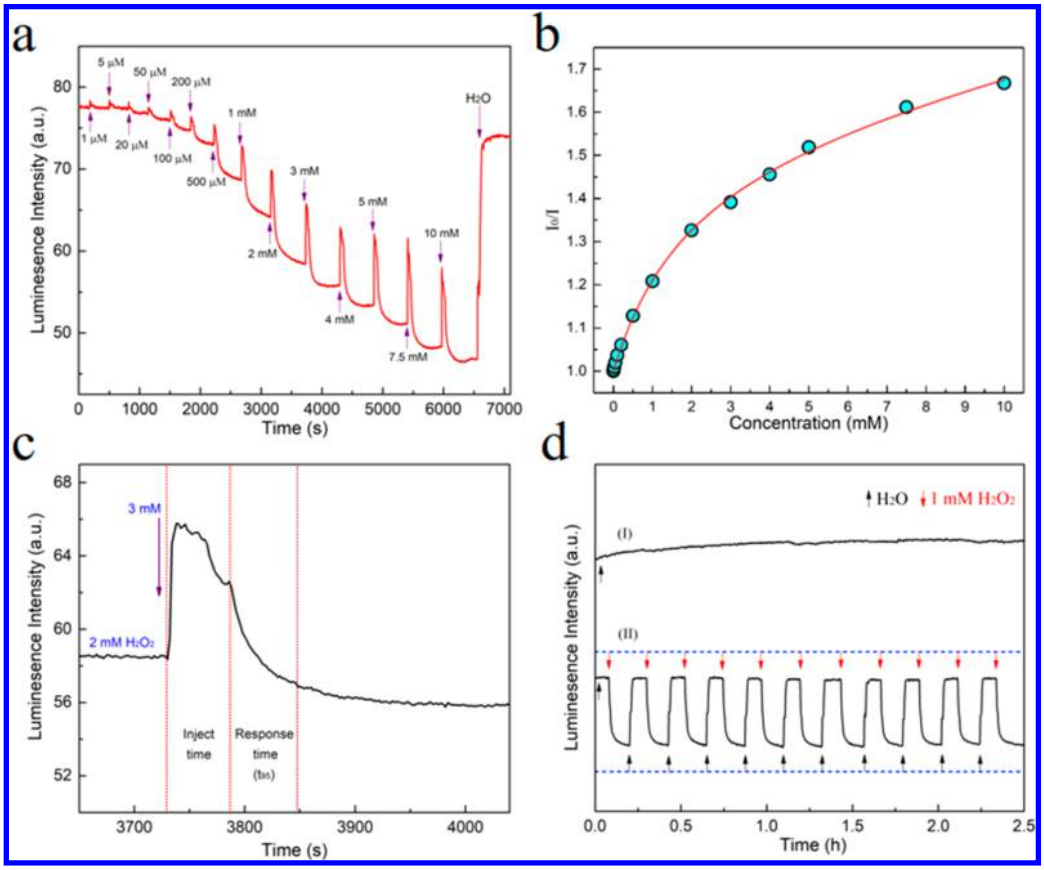

Figure 4. Response of the H_2O_2 sensor at different concentrations of H_2O_2 (a), and the corresponding Stern−Volmer plots (b), the response time of the sensor toward 3.0 mM of H_2O_2 (c), and the stability of the sensor in continuous sensing of 1.0 mM H_2O_2 for 2.5 h (d).

reversibility without loss of sensitivity over more than 2 h. Long-term study on continuously sensing of H_2O_2 also reveals the good stability of the sensor, and there is no obvious loss in sensitivity observed over a week (data not shown). Selectivity tests shown in Figure S8 in the Supporting Information show that the sensor has good selectivity to H_2O_2, and common interferences, including chloride, at high concentration (100 mM) do not influence sensor performance. An additional unexpected advantage of the sensor design is that the sensor film containing KCC-1-PEI/PtNPs composite is black in color, which can act as an optical isolation to prevent the influence of ambient light.[29,31] Because of the large size of KCC-1 particle, they also act as scatters to reflect excitation light back and forth, which is beneficial to increase the brightness of the sensor film.

DOI: 10.1021/acs.analchem.8b01159
Anal. Chem. 2018, 90, 7544−7551

Table 1. List of Reversible H_2O_2 Sensors Based on Luminescence Quenching of Oxygen

catalyst	oxygen-sensitive layer	measurement range	response time	limit of detection	remarks	ref
catalase	$Ru(dipy)_3Cl_2$ adsorbed on silica gel beads at the thickness of 50 μm		2.5−3 min	0.15 mM	two-layer system with poor stabilities in water and in dry conditions	31
silver powder	$Ru(dipy)_3Cl_2$ adsorbed on silica gel beads at the thickness of 50 μm	0.1−10 mM	3.5−5 min	0.1 mM	two-layer system with poor stabilities in water	31
MnO_2	$Ru(dpp)_3^{2+}(ClO_4^-)_2$ in polystyrene at the thickness of 40 μm	60−600 mM	797 s		three-layer system with additional poly(ether imide) covering memberane, stable over 5 days	32
RuO_2	$[Ru(bpy)_3^{2+}(Ph_4B_2)_2]$ in general purpose silicone clear at the thickness of 35 μm	0.01−1 M	309 s (t_{90})	0.1 mM	one-layer system with good reversibility	33
KCC-1-PEI/PtNPs	PtTFPP in D4 hydrogel at the thickness of 3 μm	0.001−10 mM	<1 min (t_{95})	0.015 mM	two-layer system with fast response and excellent reversibility	this work

Thinner film could be made to further reduce response time of the sensor. Besides, the sensor shows much higher sensitivity in the oxygen-free test solution (Figure S9). Because the signal change of luminescence quenching based oxygen sensors depends on the local concentration of oxygen, if the oxygen levels in the sample are very low, the signal changes will be larger than if levels of oxygen are high. This can endow the sensor extremely suitable for sensing H_2O_2 in the wastewater treatment and bleaching industry, since dissolved oxygen concentration in these occasions are lower. Thus, all these features make the sensor has outstanding response toward H_2O_2 and make real-time sensing of this chemical possible.

It has to be mentioned here that all oxygen-quenching based H_2O_2 sensors suffer from their cross sensitivity to oxygen. However, the use of additional oxygen sensor along with the H_2O_2 sensor could compensate for the influence of oxygen variation.[32] Other influences, such as temperature, can also be compensated in a similar way.

CONCLUSION

In summary, we have developed a highly sensitive, fully reversible, and reliable optical sensor for H_2O_2. The sensor was fabricated by integrating a rationally designed ultrastable and highly efficient catalytical layer onto an oxygen sensor film. The catalytical layer in the sensor rapidly converts H_2O_2 into molecular oxygen, and the concentration of decomposed oxygen was sensitively measured by the luminescence-quenching based oxygen sensor underneath. A kind of highly porous silica material (named KCC-1) with large fibrous pores is employed as carrier to the PtNPs catalyst. The large V-shape pores of KCC-1 particles not only enable direct growth of PtNPs in the channels via in situ growth strategy, but also act as dispersing and anchoring sites to protect PtNPs from aggregation and leaching. This unique structure highly enriches PtNPs catalyst and enhances the local concentration of PtNPs, which is highly favored in quick decomposing of H_2O_2 into oxygen and improving sensor sensitivity. The large V-shape pores are beneficial for molecules diffusing in and out. All these features endow the sensor exhibiting high stability, excellent reversibility, and extremely fast response (less than 1 min). The sensor can measure H_2O_2 concentration over the range from 1.0 μM to 10.0 mM. More importantly, the new H_2O_2 sensor is fully compatible with all commercial-available optical oxygen sensor devices, which makes real-time sensing of H_2O_2 in industry easier and more economically friendly.

ASSOCIATED CONTENT

Supporting Information

The Supporting Information is available free of charge on the ACS Publications website at DOI: 10.1021/acs.analchem.8b01159.

Luminescence spectra and continuous responses of PtNP (only) based H_2O_2 sensor with different PtNP concentrations and thicknesses; TEM images of PtNPs on KCC-1 with and without PEI modification; Element composition and content of KCC-1-PEI/PtNPs; Selectivity study and higher sensitivity of the H_2O_2 sensor in oxygen-free solution (PDF).

AUTHOR INFORMATION

Corresponding Author

*E-mail: wangxudong@fudan.edu.cn. Tel.: 86-021-3124 2049.

ORCID

Xu-dong Wang: 0000-0002-3402-7995

Notes

The authors declare no competing financial interest.

ACKNOWLEDGMENTS

This work was financially supported by National Key R&D Program of China (2017YFC0906800), National Natural Science Foundation of China (21775029), the Recruitment Program of Global Experts (1000 Talent program) in China, and the Program for Professor of Special Appointment (Eastern Scholar) at Shanghai Institutions of Higher Learning (No. TP2014004), which are greatly acknowledged.

REFERENCES

(1) Voraberger, H. Optical techniques for determination and sensing of hydrogen peroxide in industrial and environmental samples. In *Optical Sensors: Industrial, Environmental and Diagnostic Applications*; Narayanaswamy, R., Wolfbeis, O. S., Ed.; Springer-Verlag: Berlin, 2004; Vol. *1*, pp 391−408.

(2) Burmistrova, N.; Kolontaeva, O.; Duerkop, A. *Chemosensors* **2015**, *3*, 253−273.

(3) Stavreva, D. A.; Gichner, T. *Mutat. Res., Genet. Toxicol. Environ. Mutagen.* **2002**, *514*, 147−152.

(4) Barbouti, A.; Doulias, P. T.; Zhu, B. Z.; Frei, B.; Galaris, D. *Free Radical Biol. Med.* **2001**, *31*, 490−498.

(5) Wolfbeis, O. S.; Dürkop, A.; Wu, M.; Lin, Z. H. *Angew. Chem., Int. Ed.* **2002**, *41*, 4495−4498.

(6) Gunz, D. W.; Hoffmann, M. R. *Atmos. Environ., Part A* **1990**, *24*, 1601−1633.

(7) Satterfield, C. N.; Bonnell, A. H. *Anal. Chem.* **1955**, *27*, 1174−1175.

DOI: 10.1021/acs.analchem.8b01159
Anal. Chem. 2018, 90, 7544−7551

(8) Grau, C. A. *Bull. Sci. Pharmacol.* **1919**, *26*, 457−462.
(9) Allsopp, C. B. *Analyst* **1941**, *66*, 371.
(10) Tsiminis, G.; Chu, F.; Warren-Smith, S. C.; Spooner, N. A.; Monro, T. M. *Sensors* **2013**, *13*, 13163−13177.
(11) Venkateswaran, S. *Nature* **1931**, *127*, 406−406.
(12) Voraberger, H.; Ribitsch, V.; Janotta, M.; Mizaikoff, B. *Appl. Spectrosc.* **2003**, *57*, 574−579.
(13) Zhang, R. Z.; Chen, W. *Biosens. Bioelectron.* **2017**, *89*, 249−268.
(14) Ding, L. J.; Zhao, M. G.; Ma, Y.; Fan, S. S.; Wen, Z.; Huang, J. Y.; Liang, J. J.; Chen, S. G. *Biosens. Bioelectron.* **2016**, *85*, 869−875.
(15) Schäferling, M.; Grögel, D. B. M.; Schreml, S. *Microchim. Acta* **2011**, *174*, 1−18.
(16) Zheng, J. Y.; Yan, Y.; Wang, X.; Shi, W.; Ma, H.; Zhao, Y. S.; Yao, J. *Adv. Mater.* **2012**, *24*, OP194−OP186.
(17) Su, G.; Wei, Y. B.; Guo, M. L. *Am. J. Anal. Chem.* **2011**, *2*, 879−884.
(18) Bera, R. K.; Raj, C. R. *J. Photochem. Photobiol., A* **2013**, *270*, 1−6.
(19) Ha, T. L.; Shin, J.; Lim, C. W.; Lee, I. S. *Chem. - Asian J.* **2012**, *7*, 36−39.
(20) Choleva, T. G.; Gatselou, V. A.; Tsogas, G. Z.; Giokas, D. L. *Microchim. Acta* **2018**, *185*, 9.
(21) Lobnik, A.; Cajlakovic, M. *Sens. Actuators, B* **2001**, *74*, 194−199.
(22) Wolfbeis, O. S.; Schäferling, M.; Dürkop, A. *Microchim. Acta* **2003**, *143*, 221−227.
(23) Muhr, V.; Buchner, M.; Hirsch, T.; Jovanovic, D. J.; Dolic, S. D.; Dramicanin, M. D.; Wolfbeis, O. S. *Sens. Actuators, B* **2017**, *241*, 349−356.
(24) Hurdis, E. C.; Romeyn, H. *Anal. Chem.* **1954**, *26*, 320−325.
(25) Huckaba, C. E.; Keyes, F. G. *J. Am. Chem. Soc.* **1948**, *70*, 1640−1644.
(26) Zhu, Z.; Guan, Z. C.; Jia, S. S.; Lei, Z. C.; Lin, S. C.; Zhang, H. M.; Ma, Y. L.; Tian, Z. Q.; Yang, C. J. *Angew. Chem., Int. Ed.* **2014**, *53*, 12503−12507.
(27) Zhu, Z.; Guan, Z. C.; Liu, D.; Jia, S. S.; Li, J. X.; Lei, Z. C.; Lin, S. C.; Ji, T. H.; Tian, Z. Q.; Yang, C. J. *Angew. Chem., Int. Ed.* **2015**, *54*, 10448−10453.
(28) Quaranta, M.; Borisov, S. M.; Klimant, I. *Bioanal. Rev.* **2012**, *4*, 115−157.
(29) Wang, X. D.; Wolfbeis, O. S. *Chem. Soc. Rev.* **2014**, *43*, 3666−761.
(30) Trubel, H.; Barnikol, W. K. R. *Biomed. Tech.* **1998**, *43*, 302−309.
(31) Posch, H. E.; Wolfbeis, O. S. *Microchim. Acta* **1989**, *97*, 41−50.
(32) Voraberger, H. S.; Trettnak, W.; Ribitsch, V. *Sens. Actuators, B* **2003**, *90*, 324−331.
(33) Mills, A.; Tommons, C.; Bailey, R. T.; Tedford, M. C.; Crilly, P. J. *Analyst* **2007**, *132*, 566−571.
(34) Bayal, N.; Singh, B.; Singh, R.; Polshettiwar, V. *Sci. Rep.* **2016**, *6*, 24888.
(35) Polshettiwar, V.; Cha, D.; Zhang, X.; Basset, J. M. *Angew. Chem., Int. Ed.* **2010**, *49*, 9652−9656.
(36) Dhiman, M.; Polshettiwar, V. *J. Mater. Chem. A* **2016**, *4*, 12416−12424.
(37) Stich, M. I. J.; Fischer, L. H.; Wolfbeis, O. S. *Chem. Soc. Rev.* **2010**, *39*, 3102−3114.
(38) Amao, Y.; Miyashita, T.; Okura, I. *J. Fluorine Chem.* **2001**, *107*, 101−106.
(39) Mao, Y. Y.; Gao, Y.; Wu, S. S.; Wu, S. Y.; Shia, J. Y.; Zhou, B. P.; Tian, Y. Q. *Sens. Actuators, B* **2017**, *251*, 495−502.
(40) Fihri, A.; Cha, D.; Bouhrara, M.; Almana, N.; Polshettiwar, V. *ChemSusChem* **2012**, *5*, 85−89.
(41) Dhiman, M.; Chalke, B.; Polshettiwar, V. *ACS Sustainable Chem. Eng.* **2015**, *3*, 3224−3230.
(42) Wang, X. H.; Peng, H. S.; Yang, L.; You, F. T.; Teng, F.; Hou, L. L.; Wolfbeis, O. S. *Angew. Chem., Int. Ed.* **2014**, *53*, 12471−12475.

DOI: 10.1021/acs.analchem.8b01159
Anal. Chem. 2018, 90, 7544−7551